NUCLEAR INSTRUMENTS AND METHODS 143 (1977) 145-149 ; © NORTH-HOLLAND PUBLISHING CO.

AN ALGORITHM FOR FITTING LORENTZIAN-BROADENED, K-SERIES X-RAY PEAKS OF THE HEAVY ELEMENTS*

R. GUNNINK

Lawrence Livermore Laboratory, University of California, Livermore, California 94550, U.S.A.

Received 24 November 1976

In spectra taken with high-resolution detectors, a problem occurs in describing the line shape of K_α X-ray peaks of the heavy elements. We have now developed algorithms which adequately fit these Lorentzian-broadened distributions which are obtained by the use of Ge detectors having a full-width at half-maximum resolution of ~500 eV at 100 keV. Other aspects of X-ray and gamma-ray peak fitting are also discussed.

1. Introduction

The advent of germanium (Ge) detectors and digital computers enabled experimenters to resolve many of the features of complex gamma-ray spectra. As a result, systems with these components are used extensively to obtain accurate analytical assays of radioactive materials.

One important analytical application we have investigated is the isotopic and total analysis of plutonium-bearing materials[1,2]). One energy region, in particular, stands out as possessing a wealth of spectroscopic information for this measurement.

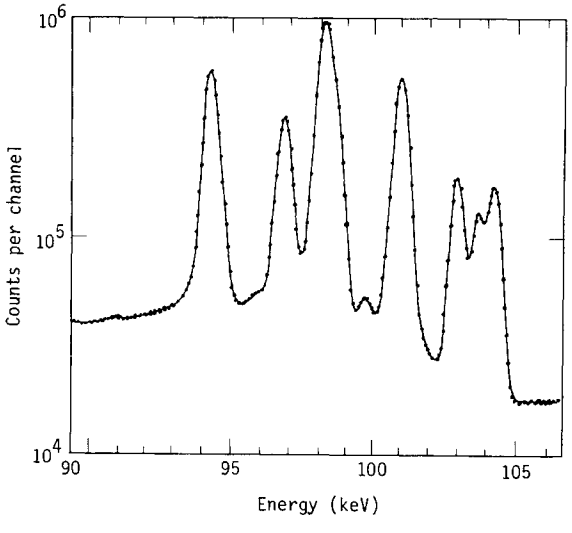

Fig. 1. The 100 keV region of a Ge spectrum of a sample of plutonium. The distribution contains up to 15 X-rays and gamma rays, many of which are unresolved.

This region, shown in fig. 1, ranges from 94 to 104 keV and contains up to 15 peaks stemming from all of the plutonium isotopes of interest plus ^{237}U and ^{241}Am.

2. Statement of the problem

The proper analysis of this complex region requires mathematical algorithms that very precisely describe the line shapes of the individual components of the grouping. We have developed such algorithms for gamma-ray peaks in a Ge spectrum[3]). However, this particular multiplet consists not only of peaks attributable to gamma rays but also of up to six peaks coming from atomic transitions that emit K_α X-rays. This presents a problem: The lifetime of these transitions is sufficiently short so that the resulting radiative width, due to the uncertainty principle*, is about 100 eV as compared to gamma-ray widths which typically are several orders of magnitude narrower. The instrumental resolution of good Ge detectors, on the other hand, is approximately 480 eV full-width at half-maximum (fwhm) at 100 keV. An additional complication is that the intrinsic X-ray line shape is Lorentzian in form[4]); whereas the prominent features of the instrumental broadening are Gaussian in shape. The resultant distribution is observed to be a convolution of these two forms of energy dispersion (see fig. 2). The attendant question is, What algorithm can be used to fit such a distribution?

The general problem has been elucidated in considerable detail by Wilkinson[5]). The purpose of this report is to show how some of the formulae

* This work was performed under the auspices of the U.S. Energy Research and Development Administration, under contract W-7405-Eng-48.

* This principle, first deduced by Heisenberg, simply states that the product of the uncertainty in the energy and the lifetime of a state must exceed the quantity $\hbar$.

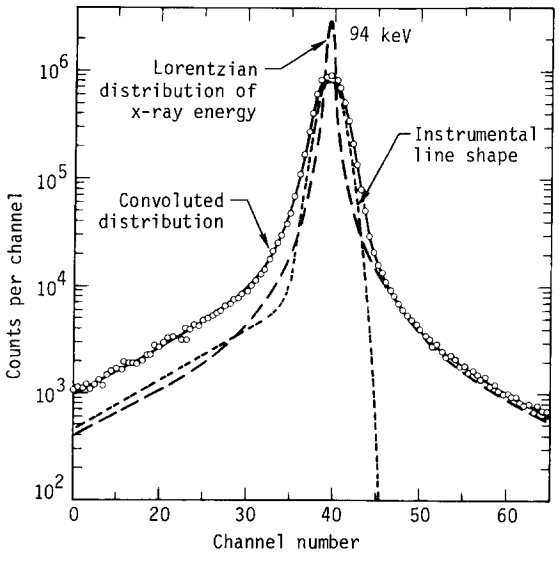

Fig. 2. The Lorentzian form for X-ray energy distribution combined with the Gaussian shape of the curve for instrumental broadening result in the convoluted distribution line shown. The resultant modified peak shape differs from that of a gamma ray of equivalent energy.

developed by Wilkinson can be implemented to resolve the problems just described.

3. Functional forms for intrinsic line shape and detector response

The X-ray line shape is given by the Breit–Wigner expression:

$$L(X) = \frac{A}{(X-X_0)^2 + (\frac{1}{2}\Gamma)^2}, \tag{1}$$

TABLE 1
Values of $\sum f(\chi) = \sum_{n=1}^{\infty} [\exp(-n^2/4)/n^2](1-\cosh n\chi)$ as a function of χ (from ref. 5).

χ (1)	$-\sum f(\chi)$ (2)	χ (3)	$-\sum f(\chi)$ (4)	χ (5)	$-e^{-\chi^2}\sum f(\chi)$ (6)
0.1	0.00638	1.6	3.454	1	0.302
0.2	0.02569	1.7	4.417	2	0.180
0.3	0.05848	1.8	5.697	3	6.15×10^{-2}
0.4	0.1057	1.9	7.430	4	3.08
0.5	0.1688	2.0	9.823	5	1.89
0.6	0.2497	2.2	18.04	6	1.29
0.7	0.3510	2.4	35.87	7	9.34×10^{-3}
0.8	0.4764	2.6	78.14	8	7.09
0.9	0.6305	2.8	187.8	9	5.58
1.0	0.8197	3.0	498.6	10	4.50
1.1	1.052	3.2	1461	11	3.71
1.2	1.340	3.4	4714	12	3.11
1.3	1.697	3.6	16686	13	2.65
1.4	2.147	3.8	64671	14	2.28
1.5	2.718	4.0	273925	15	1.98

where A is the amplitude, Γ the fwhm, and X_0 the center of the distribution. The instrumental distribution, to a first approximation, is Gaussian and, therefore, can be described by:

$$G(X) = A' \exp[\alpha(X-X_0)^2], \tag{2}$$

where $\alpha = -1/2\sigma^2$. The resulting response, known as a Voigt profile[6]), is given by

$$C(X) = A\int_{-\infty}^{\infty} \exp(\alpha X'^2)\,\frac{dX'}{(\frac{1}{2}\Gamma)^2 - (X-X'-X_0)^2}. \tag{3}$$

For the case under consideration, where Γ at fwhm is about two-tenths the instrumental resolution, the following approximate analytic expression developed by Wilkinson[5]) can be used:

$$F(X) = e^{-\chi^2}\left\{1 - \frac{\alpha}{\sqrt{\pi}}\left[1 - \frac{\chi^2}{2\sqrt{\pi}} + \frac{2}{\sqrt{\pi}}\sum f(\chi)\right] + \right.$$
$$\left. + \tfrac{1}{2}\gamma^2(1-2\chi^2)\right\}, \tag{4}$$

where

$$\chi = \sqrt{-\alpha}\cdot(X-X_0), \quad \gamma = \sqrt{-\alpha}\cdot\Gamma = 1.665\,\Gamma/\theta,$$

(θ = fwhm of instrumental resolution), and

$$\sum f(\chi) = \sum_{n=1}^{\infty}[\exp(-n^2/4)/n^2]\cdot[1-\cosh(n\chi)]. \tag{5}$$

Eq. (4) can be rewritten as:

$$F(X) = e^{-\chi^2}[C_1 + C_2\chi^2 + C_3(1-2\chi^2)] + C_4 B(\chi), \tag{6}$$

where

$$C_1 = 1 - \frac{\gamma}{\sqrt{\pi}}, \quad C_2 = \frac{\gamma}{2\pi}, \quad C_3 = 0.25\gamma^2,$$

$$C_4 = \frac{2\gamma}{\pi}, \quad \text{and} \quad B(\chi) = -e^{-\chi^2}\sum f(\chi).$$

Eq. (6) can be easily evaluated with the exception to the $B(\chi)$ term. To solve $B(\chi)$ for small values of χ, a limited number of terms of a series expansion can be used to describe $\cosh(n\chi)$. That is,

$$\cosh(n\chi) = 1 + \frac{(n\chi)^2}{2!} + \frac{(n\chi)^4}{4!} + \ldots. \tag{7}$$

An evaluation of the summation integral thus leads to:

$$\sum f(\chi) = 0.636228\cdot\chi^2 + 0.14718\cdot\chi^4 + 0.02982\cdot$$
$$\cdot\chi^6 + \ldots. \tag{8}$$

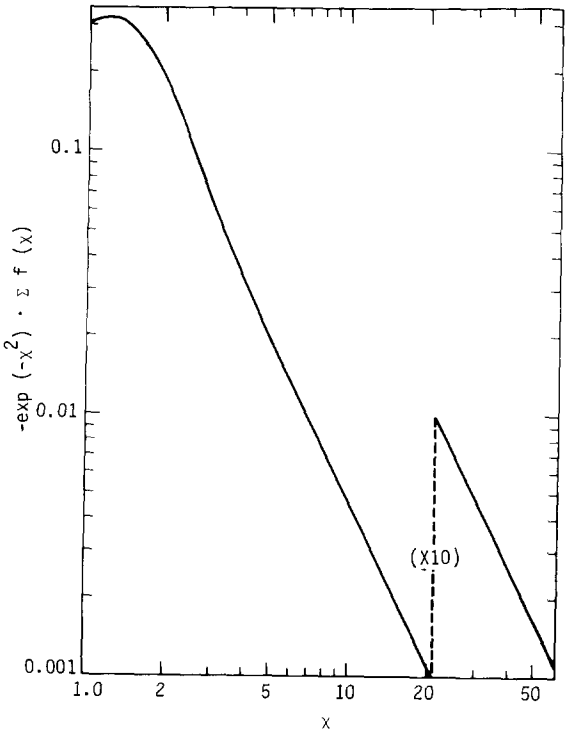

Fig. 3. In this plot of $B(\chi)$ vs χ, the part of the curve for $\chi > 2$ is easily described by a low-order polynomial.

As χ becomes larger, the above expression is no longer valid. A different method must be used to evaluate the summation integral. Table 1, taken from ref. 5 is a listing of exact values of $-\Sigma f(\chi)$ and of the product $-e^{-\chi^2}\Sigma f(\chi)$ as a function of χ. Since it appears that eq. (8), or some modification of it, can be used to describe the region corresponding to small χ, a search was made to find some suitable algorithm for calculating $B(\chi)$ for large values of χ. We found that a log–log plot of the data from the 5th and 6th columns of table 1 showed a nearly linear relationship for values of $\chi > 2$ (see fig. 3). This data region, therefore, can be fitted by the method of least squares to a polynomial of the form:

$$\ln B(\chi) = \sum_{j=1}^{n} a_j (\ln \chi)^{(j-1)}. \tag{9}$$

TABLE 2

Adjusted $\Sigma f(\chi)$ values for improved fit.

χ (1)	Adjustment factor (2)	New value of $-\Sigma f(\chi)$ (3)	χ (4)	Adjustment factor (5)	New value of $-\Sigma f(\chi)$ (6)
0.1	1.088	0.006941	1.2	1.049	1.405
0.2	1.088	0.02795	1.3	1.043	1.769
0.3	1.087	0.06357	1.4	1.037	2.225
0.4	1.085	0.1147	1.5	1.031	2.801
0.5	1.083	0.1828	1.6	1.025	3.540
0.6	1.080	0.2696	1.7	1.020	4.505
0.7	1.075	0.3775	1.8	1.015	5.780
0.8	1.070	0.5100	1.9	1.010	7.504
0.9	1.065	0.6718	2.0	1.006	9.882
1.0	1.060	0.8689	2.2	0.999	18.02
1.1	1.055	1.109	2.4	0.995	35.69

4. Evaluation of the functions

Two questions which now arise are: How well does eq. (6) and its variations, expressed by eqs. (8) and (9), describe X-ray peak shapes and for what set of values of χ should each functional form be used?

To help answer these and related questions, we wrote a computer program to generate Voigt profiles. The procedure assumes that an experimentally measured gamma-ray distribution can be used to determine the instrumental smearing at any given energy. The intrinsic Lorentzian-shaped X-ray distribution was divided into 15 eV segments, with each segment smeared according to the measured instrumental distribution. A numerical integration at each point (channel) finally produces a convoluted profile of the two distributions.

The results of initial attempts at using eqs. (8) and (9) for describing the generated Voigt profiles indicated a reasonable fit, but they also showed some definite anomalies (fig. 4). An examination of the deviations revealed some of the causes. First, eq. (4) is only an approximation, and Wilkinson[5]) predicts that non-statistical deviations of $\pm 1\%$ can be expected for the case we are considering. Indeed, for small values of χ and where eq.

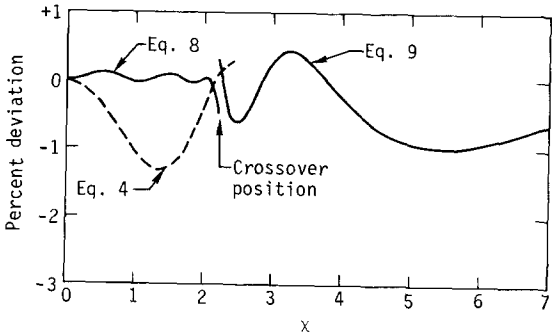

Fig. 4. Deviations between calculated and Voigt-generated profiles. Significant improvement is obtained in the vicinity of the peak centroid when eqs. (8) and (9) are used.

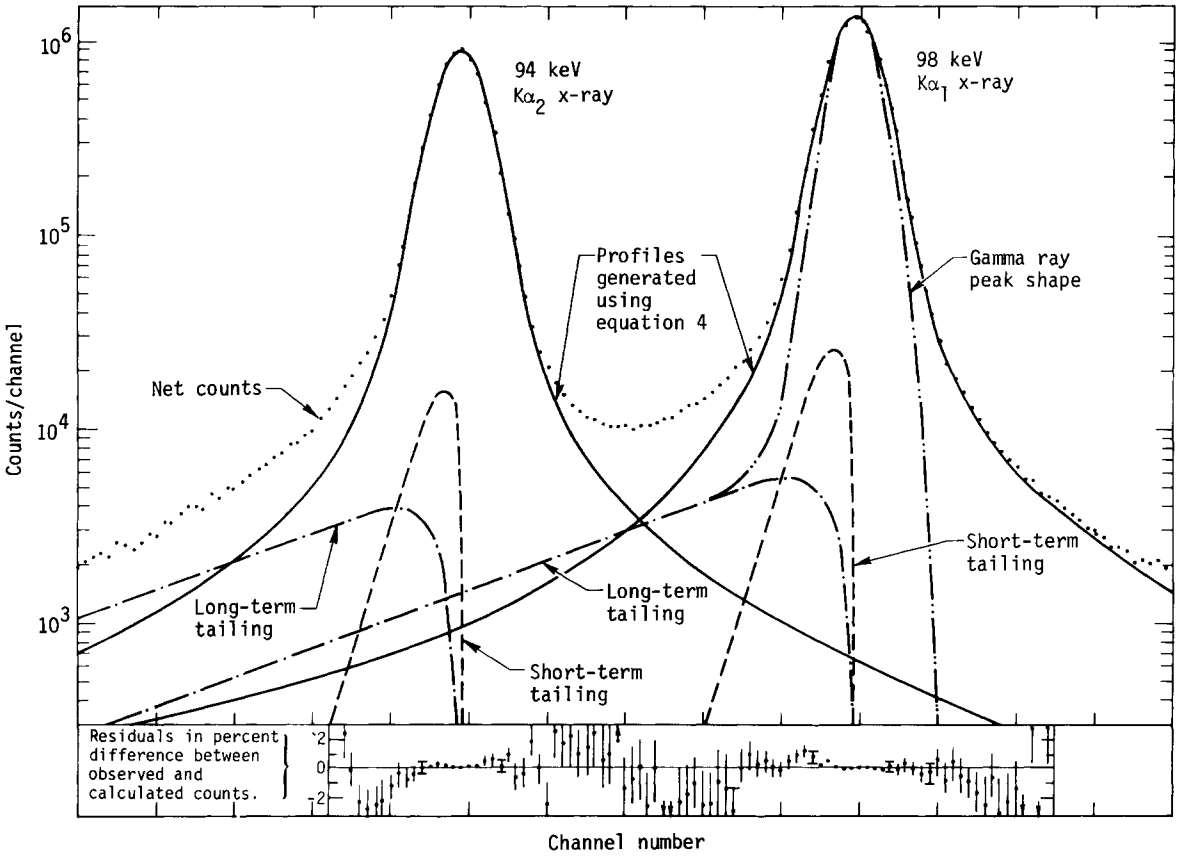

Fig. 5. The $K_{\alpha 1}$–$K_{\alpha 2}$ X-ray peaks of uranium obtained with a Ge detector. Note the component distributions used to describe the observed data. The residual data show the precision of fitting that can be obtained using eqs. (6), (8), and (9).

(8) is used, the observed and predicted deviations correlate very well. We also noted that the deviations, in effect, could be eliminated by systematically changing the computed values of the $-\sum f(\chi)$ integral. Column 2 of table 2 shows the calculated adjustment factors needed to produce the correct results. Since eq. (8) is simply a polynomial equation in χ^2, it is possible to generate a new set of coefficients which combine the small corrections necessary to achieve a good fit with the intrinsic description of the $-\sum f(\chi)$ function. This can be done using the adjusted set of values for $-\sum f(\chi)$ (table 2). For higher values of χ and where eq. (9) is used, the principal source of error can be attributed to the fact that this equation is not a rigorous description of the set of data in the 5th and 6th columns of table 1. The final sets of coefficients for eqs. (8) and (9) are given in table 3. A value of $\chi = 2.2$ was selected as the optimum cross-over position.

TABLE 3

Table of coefficients for eqs. (8) and (9).

Eq. (8)	Eq. (9)
0.729281	0.933301
0.0344557	−4.45603
0.127639	1.16191
−0.0325239	−0.141124
0.00642257	−0.0352464
	0.00744387

Using the newly-modified forms of eqs. (8) and (9), the generated Voigt profile could be fitted within a few tenths of a percent for small values of χ and to within 1% for larger values, with deviation patterns as shown in fig. 4.

The ultimate test of the usefulness of these new functional forms is their ability to describe the line shape characteristics of experimentally derived X-ray peaks. In order to perform such a test, a sample of ^{235}Np was counted using a Ge(Li) detector

with a resolution of 480 eV fwhm at 100 keV. This source was chosen because its only emissions are uranium X-rays due to decay by the electron-capture process. Counts of over 10^6 per channel at the peak centroid were obtained using a system gain of 0.075 keV/channel. The net counts of the resulting $K_{\alpha 1}$ and $K_{\alpha 2}$ X-ray distributions are plotted in fig. 5. This figure also shows the various components used to analytically describe the composite distribution.

Two important points must be made regarding the fitting of experimental distributions. First, the observed X-ray distribution is not only a convoluted response of Lorentzian and Gaussian profiles but also contains some tailing of these profiles toward lower energies. In our investigation of this problem using pure gamma-ray peaks, we have identified both a long- and a short-term tailing component[2]). The total tailing component, $T(x)$, can be described using the following algorithm:

$$T(x) = \underbrace{[A \exp(Bx)}_{\text{Short-term tailing}} + \underbrace{C \exp(Dx)]}_{\text{Long-term tailing}} \times$$

$$\times [1 - \exp(0.4\alpha x)]\, \delta\,, \qquad (10)$$

where A and C are amplitude parameters and B and D govern the slope of the tailing. The final term involving α reduces the effect of the algorithm to zero at the peak position, and δ, which has a value of either 1 or 0, keeps the algorithm at zero for positive values of x.

The second important consideration brought out by fig. 5 is that it is very difficult to determine channel positions which describe the onset and termination of an X-ray peak. In practice, we have found it necessary to select, rather arbitrarily, background regions at either end of a peak or peak grouping. However, it is important that the chosen backgrounds be corrected for the remaining peak and tailing contributions to these selected regions. This can be done by making a priori estimates of the peak heights, computing the respective contributions to the background regions, and then making the corresponding adjustments. One iteration of this process is generally sufficient.

When these adjustments are properly implemented, we have found that the given descriptions, eqs. (4) and (10), adequately fit the experimentally derived X-ray distribution. In fig. 5, errors of only a few tenths of a percent are observed in the immediate vicinity of the peak centroid, and deviations elsewhere are less than 1–2%.

These algorithms have become the basis of programs which now are used successfully to analyze complex peak regions such as shown in fig. 1. Even minor and invisible components can now be quantitatively measured when sufficient counts are accumulated.

References

[1]) R. Gunnink, J. B. Niday and P. D. Siemens, Lawrence Livermore Laboratory, Livermore, Calif., Rept. UCRL-51577 (1974).

[2]) R. Gunnink, Lawrence Livermore Laboratory, Livermore, Calif., Rept. UCRL-74618, (1975).

[3]) R. Gunnink and J. B. Niday, Lawrence Livermore Laboratory, Livermore, Calif., Rept. UCRL-51061 (1971).

[4]) V. Weisskopf and E. Wagner, Z. Physik **63** (1930) 54.

[5]) D. L. Wilkinson, Nucl. Instr. and Meth. **95** (1971) 259.

[6]) R. L. Roberts, R. A. J. Riddle and G. T. A. Squier, Nucl. Instr. and Meth. **130** (1975) 559.